

## A DFT Investigation of Tris-(4'-(Amino)(1,1'-biphenyl)-3,4-diol) Fe(III) Complex

Mohammad A. Matin<sup>1</sup>, Mohammed A. Aziz<sup>2</sup> and M. Saiful Islam<sup>\*2</sup>

<sup>1</sup>Centre for Advanced Research in Sciences (CARS), Dhaka University, Dhaka, Dhaka-1000, Bangladesh

<sup>2</sup>Department of Theoretical and Computational Chemistry, Dhaka University, Dhaka-1000, Bangladesh

( Received: 3 December 2017 ; Accepted : 16 January 2018)

### Abstract

Phenolic compounds, known as the pyrocatechol act as a metal chelating agent. Molecular details of cross-linking of pyrocatechol by transition metal ions are largely unknown. In the present study, the molecular properties of the tris-(4'-(amino)(1,1'-biphenyl)-3,4-diol)-Fe(III) complex have been investigated using density functional theory (DFT) at 6-311G(d,p). Calculated molecular properties of the optimized structure, the binding energies and spectroscopic properties are compared with the available experimental results. For the tris-complex investigated, the binding of Fe (III) with the catechol derivative is not as strong as the binding of other metal ions with catechol. The IR stretching bands show that the strong IR intensities is due to large charge polarization. Calculated electronic band gap is 2.45 eV which is in the range of transition metal ion-tris-(4'-(amino)(1,1'-biphenyl)-3,4-diol) complexes. The metal-ligand binding energy is 513.54 kcal mol<sup>-1</sup>, which could be used in understanding the speciation of Fe(III)-catechol complex. Structural parameters obtained from the DFT calculations are in good agreement with the crystallographic data.

**Keywords:** Tris-(4'-(amino)(1,1'-biphenyl)-pyrocatechol, Density Functional Theory, Electronic properties.

### I. Introduction

The ligand (4'-(amino)(1,1'-biphenyl)-3,4-diol) is one of the phenolic compounds known as pyrocatechol, acts as iron chelating agent<sup>1,2</sup>. Pyrocatechol, in alkaline solution reacts with iron ion and forms [Fe(cat)<sub>3</sub>]<sup>n-</sup> complexes, (where n=1, 2 and 3) which have been used for the treatment of human metal intoxication<sup>2</sup>. The binding of iron ion with catechol derivatives and other chelating agents are an important area of research activities. A good understanding of the metal ion pyrocatechol complexes may play an important role in determining the speciation of Fe(III), chelating complexes in its biological activity<sup>3</sup>.

An adequate supply of iron is necessary for optimal plant productivity and their quality<sup>4</sup>. Iron is important for the correct functioning of all living cells on one hand, whereas on the other hand, presence of excess iron causes the toxicity. Excess iron may originate from the aggregation of iron in the body. This aggregation of iron maybe reduced by the iron chelating. Several researchers have attempted to obtain a clear understanding of Fe(III)-catechol interaction mechanism<sup>5,6</sup>.

Experimental work showed that the coordination between Fe(III) and (4'-(amino)(1,1'-biphenyl)-3,4-diol) ligand is strongly pH dependent<sup>7</sup> and in Fe(III)-catechol cross-link polymer, Fe(III) does not affect a significant covalent cross-linking via oxidation of catechol. However, spectroscopic studies have linked the presence of Fe(III) to catechol oxidation<sup>8-10</sup>. Fe (III) ion mediate the cross-linking of modified catechol in acidic pH<sup>11-12</sup>. Therefore, an extensive study of the mechanism of interactions between Fe(III) and (4'-(amino)(1,1'-biphenyl)-3,4-diol) catechol derivative is necessary.

There have been only a limited number of theoretical studies of Fe(III) complexes of catechol<sup>13</sup>. Liu *et al.* have simulated the Fe(III)-DOPA mediated bridging at both the gas phase

and in aqueous solution<sup>14-15</sup> at the B3LYP/LACVP(d) level. To date, no theoretical investigation of the [Fe(4'-(amino)(1,1'-biphenyl)-3,4-diol)<sub>3</sub>]<sup>3-</sup> complex has been reported as far known to us. We have performed the calculation on the complex to provide a detailed investigation on the structures, binding energy and spectroscopic properties. The natural bond orbital (NBO) analysis<sup>16</sup> and analysis of the frontier MO energies (HOMO and LUMO) along with the corresponding energy gap have been done and reported here.

### II. Computational Method

Density functional theory (DFT) calculations were carried out with Gaussian09 package<sup>17</sup>. All structures in this study were fully optimized in the gas phase and in solvent (water) using PCM at B3LYP level of theory. For, C, H, N and O atoms, 6-311G (d, p) basis set and for Fe, LANL2DZ basis set were employed. Vibrational frequencies of the optimized structure were obtained to check for the absence of any imaginary frequencies. Gauss View 5.0.8 program was used for the visualization of the optimized structures and simulated vibrational spectra. The metal ion-ligand binding energy was calculated according to the equation

$$\Delta E = \frac{[(E_{\text{complex}} - (E_{\text{metal}} + E_{\text{ligand}})]}{3}$$

where  $E_{\text{complex}}$ ,  $E_{\text{metal}}$  and  $E_{\text{ligand}}$  are the energies of the tris-(4'-(amino)(1,1'-biphenyl)-3,4-diol)Fe(III) complex, the metal ion and isolated ligand (4'-(amino)(1,1'-biphenyl)-3,4-diol), respectively.

The IR frequencies of the complex were calculated using the analytic gradient and Hessian. Scaling of computed vibrational frequencies by 0.9668 was found good agreement with experimental results<sup>18</sup>. Analysis of the frontier MO have been done by finding the energy gap between the HOMO and LUMO.

\* Author for correspondence. e-mail: dr.mdsaufislam@yahoo.com

### III. Results and Discussion

#### Structural parameters

Calculated structural parameters for the optimized structure of the tris-(4'-amino-(1, 1'-biphenyl)-3, 4-diol)-Fe (III) complex (Figure 1) in the gas phase are presented in the Table 1 along with the available corresponding X-ray data of the complex. The agreement between the calculated and experimental structural parameters are good. The calculated value for the O-Fe-O angles indicate near octahedral geometry around the Fe(III) ion in the complex.

Previous DFT study<sup>19</sup> on  $[\text{Fe}(\text{cat}^2)_3]^{3-}$  and X-ray analysis of the tris-catecholate-Fe (III) complex (The  $\text{K}_3 [\text{M}(\text{cat})_3] \cdot 1.5\text{H}_2\text{O}$  complex where  $\text{M}=\text{Cr}, \text{Fe}$ )<sup>20</sup> reported Fe (III)-O distances of 2.05 and 2.015 Å, respectively. Therefore the present Fe(III)-O distances are close to these theoretical and experimental values.

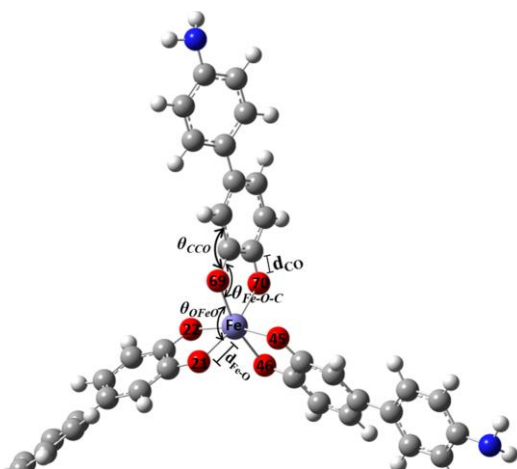


**Fig. 1.** Optimized structure of the tris-(4'-(amino)(1,1'-biphenyl)-3,4-diol)-Fe(III) complex.

The present O-Fe-O angle is significantly larger by 9.29° than the previous<sup>20</sup> X-ray crystal structure, 81.13°. Another DFT study on a monocatecholate Fe(III) complex<sup>21</sup> reported a Fe-O distance and O-Fe-O angle of 1.933 Å and 86.5°, respectively.

#### Vibrational spectra of the complex

IR spectrum of the complex obtained by the quantum chemical calculation in this work is shown in the Figure 2 and the vibrational frequencies are given in the Table 2. Two intense peaks at 1288 and 1456  $\text{cm}^{-1}$  are observed.

Each of these two major intense peaks has originated from the in-plane deformation mode involving the C-C and C-O stretching and the C-H bending of the biphenyl pyrocatecholate, which is in the good agreement with the experimental results<sup>22</sup>.

**Table 1. Structural parameters of the optimized tris-(4'-amino-(1,1'-biphenyl)-3,4-diol)-Fe(III) complex.**

	Calculated (this work)	Expt <sup>20</sup>
Bond distances (Å)		
Fe-O	2.074	2.015
C-O	1.296	1.349
Bond angles (°)		
O-Fe-O	90.42	81.13
C-C-O	125.16	123.9
Fe-O-C	114.71	112.0

The O-Fe stretching ( $\nu\text{Fe-O}$ ) was observed in the range of 401-651  $\text{cm}^{-1}$ . The stretching frequencies at 570  $\text{cm}^{-1}$  and 634  $\text{cm}^{-1}$  are originated from the interaction between Fe(III) ion and  $\text{C}_3$  and  $\text{C}_4$  oxygens (here the two carbon atoms that attached with oxygens are denoted as  $\text{C}_3$  and  $\text{C}_4$ ) of the pyrocatecholate respectively.

**Table 2. Selected IR data of the optimized complex obtained at B3LYP/6-311G(d,p).**

Assignments	Scaled frequencies/ $\text{cm}^{-1}$	Expt. <sup>22</sup>
$\delta, \nu\text{Fe-O}$	520	530( $\nu\text{Fe-O}$ )
$\nu\text{Fe-O}$	570	-
$\nu\text{Fe-O}$	634	636( $\nu\text{Fe-O}$ )
$\delta\text{CCH}$	1149	1164( $\nu\text{CO}+$ $\nu\text{CC}$ )
$\nu\text{CC}$	1288	-
$\nu\text{CO}+\delta\text{CCH}$	1332	1387( $\nu\text{C-O}$ )
$\nu\text{CC}+\delta\text{CCH}$	1456	1439( $\nu\text{CC}$ )
$\nu_{\text{asym}}\text{C-H}$	3083	-
$\nu_{\text{sym}}\text{N-H}$	3347	-
$\nu_{\text{asym}}\text{N-H}$	3437	-

Fe means Fe(III) ion.

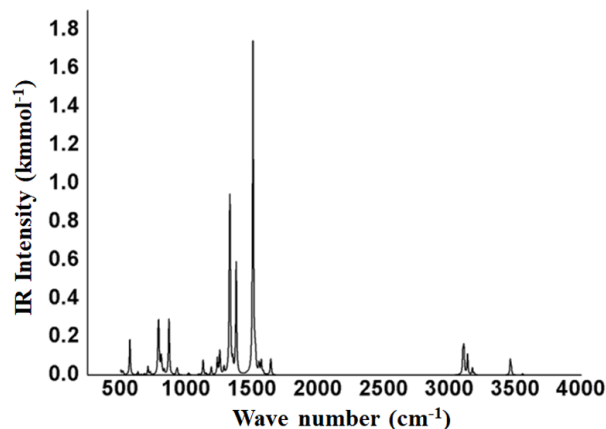


**Fig. 2.** Theoretical IR spectrum of tris-(4'-(amino)(1,1'-biphenyl)-3,4-diol)-Fe(III) complex.

The intense  $\nu\text{Fe(III)-O}$  band experimentally observed<sup>22</sup> at  $636\text{ cm}^{-1}$ . The C-O stretching ( $\nu\text{C-O}$ ) vibrational frequencies of the complex were obtained in the range of  $1283\text{-}1517\text{ cm}^{-1}$ . The most intense vibrations of the  $\nu\text{C-O}$  as symmetric frequency at  $1332\text{ cm}^{-1}$  and the  $\nu\text{C-C}$  aromatic ring vibrations were observed at  $1456\text{ cm}^{-1}$ . The  $\nu\text{C-H}$  aliphatic vibrations were found in the range of  $3043\text{ cm}^{-1}$ . The  $\nu_{\text{sym}}\text{NH}$  and  $\nu_{\text{asym}}\text{NH}$  vibrations were in  $3347$  and  $3437\text{ cm}^{-1}$  respectively. The high intensities of IR peaks obtained in this work occur because of the highly positive iron ion surrounded by the negatively charged oxygen of the ligands

#### Analysis of frontier molecular orbital (MO)

To characterize the electronic transitions of the complex, two frontier molecular orbitals (MOs) are illustrated in the Figure 3, highest occupied molecular orbital (HOMO) and the lowest unoccupied molecular orbital (LUMO). In the HOMO, the electrons are distributed mainly over three pyrocatecholate ligands. Strong metal ligand delocalization is found to occur between two of the three ligands in each case. An electronic system with a larger HOMO-LUMO gap should be less reactive than one having a smaller gap<sup>23</sup>. The HOMO-LUMO gap of this model complex is  $2.45\text{ eV}$ . This higher HOMO-LUMO gap indicates the weaker complex between Fe(III) ion and the ligand studied in this work.

#### Charges on the metal ion in the complex

The charge on the ion obtained from four different schemes is given in the Table 3. These schemes are natural population analysis, NPA<sup>24</sup>, Merz-Singh-Kollman scheme, MK<sup>25</sup>, CHarges from Electrostatic Potentials with grid oriented, CHelpG<sup>26</sup> and

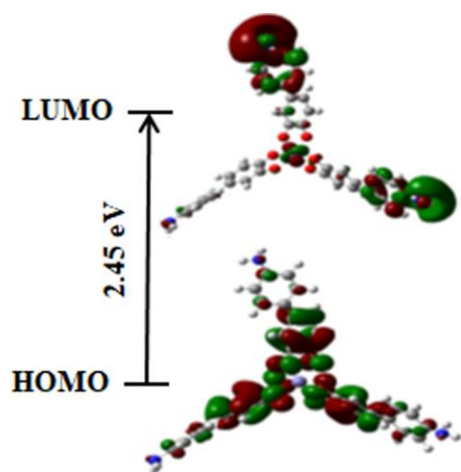


**Fig. 3.** Frontier MOs for the optimized complex. The isosurface value is  $0.02\text{ electrons Bohr}^{-3}$ .

CHarges from Electrostatic Potentials CHelpG<sup>27</sup>. Charges on the ion in the complex obtained by NPA and MK scheme are very close, but the charge obtained by CHelpG method is higher by  $0.172$ . However, the charge obtained by CHelp method is overestimated by  $0.459$ .

**Table 3.** Charges on the metal ion at various charge schemes and binding energy ( $\Delta E$ ) of the complex.

Charge	$\Delta E(\text{kcal mol}^{-1})$	
	This work	Reference <sup>28</sup>
1.304(NPA), 1.295(MK), 1.467 (CHelpG)	513.54	540.05-553.41
1.754(CHelp)		

#### Binding energy and the solvent effect

We have investigated the metal ion-ligand binding energy ( $\Delta E$ ) and is given in the Table 3 obtained in this work. The calculated metal ion binding energy ( $513.54\text{ kcal mol}^{-1}$ ) obtained in this work is very close to those of the metal ion hexa-aqua complexes ( $540.05$  to  $553.41\text{ kcal mol}^{-1}$ )<sup>28</sup>.

We also investigated the solvent effects for the Fe(III) complex by employing the conductor-like polarizable continuum model (CPCM)<sup>29-30</sup>. The energy of metal ion – ligand complex is virtually unchanged in a water solvent, only varying by less than  $0.018\%$  (Table 4). The structural change of the complex due to the presence of the solvent was neglected in this calculation. However, we considered that the near octahedral geometry around the central metal ion of the complex remains unchanged with the introduction of the solvent. Therefore, the present metal-ligand binding energy presumably will not deviate much from those in the solvent.

**Table 4.** Solvent effect on the metal complex.

Metal complex	Electronic energy/a.u.	Electronic energy(sol. Phase) <sup>a</sup> /a.u.	Solvent effect/ kcal mol <sup>-1</sup>	%Relative deviation
Fe(III)	-2127.71	-2127.32	-244.73	0.018

<sup>a</sup>gas phase optimized geometry was taken.

#### Natural Bond Orbital (NBO) analysis

NBO calculations provides a reasonable picture from the structural, energetic, bonding and stereo electronic points of view<sup>31</sup>. DFT level computation is used to investigate the various second-order inter-actions between the filled orbitals of one subsystem and vacant orbital of another subsystem<sup>32</sup>. The relevant NBO of the complex are collected in the Table 5. Inspection of this results indicate that interaction between the lone pair orbitals of the oxygen of the pyrocatecholate ligand and the iron ion ( $\text{LP}_{\text{O}22} \rightarrow \text{LP}_{\text{Fe}}$ ) is about  $16.92\text{ kcal mol}^{-1}$ , relatively stronger. The interactions  $\text{LP}_{\text{O}46} \rightarrow \text{LP}_{\text{Fe}}^*$  and  $\text{LP}_{\text{O}70} \rightarrow \text{LP}_{\text{Fe}}^*$  are  $14.01$  and  $14.54\text{ kcal mol}^{-1}$  respectively. The most important interaction energies of the complex are due to the interactions between the lone pair(LP) electrons of the O atom ( $\text{LP}_{\text{O}}$ ) and antibonding orbital of the Fe(III)( $\text{LP}_{\text{Fe}}^*$ ). These results given in the Table 5 clearly shows that the relative intense  $\text{LP}_{\text{O}} \rightarrow \text{LP}_{\text{Fe}}^*$  hyperconjugative interaction plays an important role in stabilizing the complex, thus enabling the formation of octahedral complex.

**Table 5. Energies of orbitals interactions (in kcal mol<sup>-1</sup>) of the optimized complex in the gas phase.**

Interaction	$E_{\text{NBO}}$ (kcal mol <sup>-1</sup> )
LP <sub>O21</sub> →LP* <sub>Fe</sub>	13.17
LP <sub>O22</sub> →LP* <sub>Fe</sub>	16.92
LP <sub>O45</sub> →LP* <sub>Fe</sub>	13.19
LP <sub>O46</sub> →LP* <sub>Fe</sub>	14.01
LP <sub>O69</sub> →LP* <sub>Fe</sub>	13.08
LP <sub>O70</sub> →LP* <sub>Fe</sub>	14.54
LP <sub>N23</sub> →BD* <sub>C5-C6</sub>	6.76
LP <sub>N47</sub> →BD* <sub>C-28-C29</sub>	6.65
LP <sub>N71</sub> →BD* <sub>C52-C53</sub>	7.35

BD\* =bonding electrons, LP=lone pair, Fe\*=Fe(III)

#### IV. Conclusion

A complete description of the geometrical parameters, spectroscopic, electronic properties of the tris-(4'-amino-(1, 1'-biphenyl)-3, 4'-diolate)-Fe(III) complex was performed theoretically using DFT level of the theory. The present study will be helpful to understand the structure of the tris-(4'-amino-(1, 1'-biphenyl)-3, 4'-diolate)-Fe(III) complex for studying the metal ion-ligand interaction. The optimized bond distances and bond angles are in well accord with the experimental data<sup>20</sup>. The simulated IR spectra of the model compound are all consistent with the previous measurements. The calculated binding energy, structural parameters and atomic charges can be a good approximation for further study by molecular dynamics or Monte Carlo simulation.

#### References

- Katoh, S., J. Toyama, I. Kodama, K. Kamiya, T. Akita, and T. Abe, 1992 Protective Action of Iron-Chelating Agents (Catechol, Mimosine, Deferoxamine, and Kojic Acid) against Ischemia-Reperfusion Injury of Isolated Neonatal Rabbit Hearts, *European Surgical Research*, **24**, 349-355.
- Xu, G., C. Yang, B. Liu, X. Wu, and Y. Xie, 2004. Synthesis of New Potential Chelating Agents: Catechol-Bisphosphonate Conjugates for Metal Intoxication Therapy. *Heteroatom Chemistry*, **15**, 251-257.
- Crichton, R., 2016. *Iron Metabolism: From Molecular Mechanisms to Clinical Consequences*, John Wiley & Sons, Hoboken.
- Briat, J.F., C. Dubos, and F. Gaymard, 2015. Iron Nutrition, Biomass Production, and Plant Product Quality, *Trends Plant Science*, **20**, 33-40
- Krogsgaard, M., M. A. Behrens, J. S. Pedersen, and H. Birkedal, 2013. Self-Healing Mussel-Inspired Multi-pH responsive Hydrogels, *Biomacromolecules*, **14**, 297-301.
- Brubaker, C. E., H. Kissler, L. J. Wang, D. B. Kaufman, and P. B. Messersmith, 2010. Biological Performance of Mussel-inspired Adhesive in Extra hepatic Islet Transplantation, *Biomaterials*, **31**, 420-427.
- Xu, C., K. Xu, H. Gu, R. Zheng, H. Liu, X. Zhang, Z. Guo, and B. Xu, 2004. Dopamine as a Robust Anchor to Immobilize Functional Molecules on the Iron Oxide Shell of Magnetic Nanoparticles, *J. Am. Chem. Soc.*, **126**, 9938-9939.
- Harrington, M. J. and J. H. Waite, 2007. Holdfast Heroics: Comparing the Molecular and Mechanical Properties of *Mytilus Californianus* Byssal Threads, *J. Expt. Biol.*, **210**, 4307-4318.
- Mentasi, E. and E. Pelizzetti, 1973. Reactions between Iron(III) and Catechol(O-Dihydroxybenzene). Part I. Equilibria and Kinetics of Complex Formation in Aqueous Acid Solution, *J. Chem. Soc., Dalton Transaction*, **23**, 2605-2608.
- Mentasi, E., E. Pelizzetti, and G. Saini, 1973. Reactions between Iron(III) and Catechol (O-Dihydroxybenzene). Part II. Equilibria and Kinetics of the Redox Reaction in Aqueous Acid Solution, *J. Chem. Soc., Dalton Transaction*, **23**, 2609-2614.
- Barrett, D. G., D. E., Fullenkamp, L. He, N. Holten-Andersen, K. Y. C. Lee, and P.B. Messersmith, 2013. pH-Dependent Regulation of Hydrogel Mechanical Properties through Mussel-Inspired Chemistry and Processing, *Adv. Funct. Mater.* **23**, 1111-1119.
- Fullenkamp, D. E., D. G. Barrett, D. R. Miller, J. W. Kurutz, and P. B. Messersmith, 2014. pH-Dependent Cross-Linking of Catechols through Oxidation via Fe<sup>3+</sup> and Potential Implications for Mussel Adhesion, *RSC Advances*, **4**, 25127-25134.
- Šebestík, J., M. Šafařík, and P. Bouř, 2012. Ferric Complexes of 3-Hydroxy-4-Pyridinones Characterized by Density Functional Theory and Raman and UV-Vis Spectroscopies, *Inorg. Chem.*, **51**, 4473-4481.
- Matin, M.A., R. K. Chitumalla, M. Lim, X. Gao, and J. K. Jang, 2015. Density Functional Theory Study on the Cross-Linking of Mussel Adhesive Proteins, *J. Phys. Chem. B*, **119**, 5496-5504.
- Liu, Q., X. Lu, H. Zhang, G. Liu, H. Zhong, and H. Zeng, 2016. Probing the Reversible Fe<sup>3+</sup>-DOPA-Mediated Bridging Interaction in Mussel Foot Protein-1, *J. Phys. Chem. C*, **120**, 21670-21677.
- Weinhold, F. and C. R. Landis, 2001. Natural Bond Orbitals and Extensions of Localized Bonding Concepts, *Chem. Edu. Res.*, **2**, 91-104.
- Frisch M. J., G.W. Trucks, H.B. Schlegel, G.E. Scuseria, M.A. Robb, J.R. Cheeseman, G. Scalmani, V. Barone, B. Mennucci, G.A. Petersson, H. Nakatsuji, M. Caricato, X. Li, H.P. Hratchian, A.F. Izmaylov, J. Bloino, G. Zheng, J.L. Sonnenberg, M. Hada, M. Ehara, K. Toyota, R. Fukuda, J. Hasegawa, M. Ishida, T. Nakajima, Y. Honda, O. Kitao, H. Nakai, T. Vreven, J.A. Montgomery Jr., J.E. Peralta, F. Ogliaro, M. Bearpark, J.J. Heyd, E. Brothers, K.N. Kudin, V.N. Staroverov, R. Kobayashi, J. Normand, K. Raghavachari, A. Rendell, J.C. Burant, S.S. Iyengar, J. Tomasi, M. Cossi, N. Rega, N.J. Millam, M. Klene, J.E. Knox, J.B. Cross, V. Bakken, C. Adamo, J. Jaramillo, R. Gomperts, R.E. Stratmann, O. Yazyev, A.J. Austin, R. Cammi, C. Pomelli, J.W. Ochterski, R.L. Martin, K. Morokuma, V.G. Zakrzewski, G.A. Voth, P. Salvador, J.J. Dannenberg, S. Dapprich, A.D. Daniels, O. Farkas, J.B.

- Foresman, J.V. Ortiz, J. Cioslowski, D.J Fox, Gaussian, Inc., Wallingford CT, 2009.
18. Merrick, J. P., D. Moran, and L. Radom, 2007. An Evaluation of Harmonic Vibrational Frequency Scale Factors, *J. Phys. Chem. A*, **111**, 11683-11700.
  19. Horsman, G. P., A. Jirasek, F. H. Vaillancourt, C. J. Barbosa, A. A. Jarzecki, C. Xu, Y. Mekmouche, T. G. Spiro, J. D. Lipscomb, M. W. Blades, et al. 2005. Spectroscopic Studies of the Anaerobic Enzyme-Substrate Complex of Catechol 1,2-Dioxygenase, *J. Am. Chem. Soc.*, **127**, 16882-16891.
  20. Raymond, K. N., S. S. Isied, L. D. Brown, F. R. Fronczek, and J. H. Nibert, 1976. Coordination Isomers of Biological Iron Transport Compounds. VI. Models of the Enterobactin Coordination Site. A Crystal Field Effect in the Structure of Potassium Tris(catecholato)-chromate(III) and -Ferrate(III) Sesquihydrates,  $K_3[M(O_2C_6H_4)_3] \cdot 1.5H_2O$ , *M = Chromium, Iron*, *J. Am. Chem. Soc.*, **98**, 1767-1774.
  21. Öhrström, L., I. Michaud-Soret, 1999. Fe-Catecholate and Fe-Oxalate Vibrations and Isotopic Substitution Shifts from DFT Quantum Chemistry, *J. Phys. Chem. A*, **103**, 256-264.
  22. Barreto, W. J., S.R.G. Barreto, I. Moreira, Y. Kawano, 2006. Iron Oxide and Pyrocatechol: A Spectroscopy Study of the Reaction Products, *Quim Nova*, **29(6)**, 1255-1258.
  23. Nono, H. J., D. B. Mama, J. N. Ghogomu, and E. Younang, 2017. A DFT Study of Structural and Bonding Properties of Complexes Obtained from First-Row Transition Metal Chelation by 3-Alkyl-4-phenylacetyl-amino-4,5-dihydro-1H-1,2,4-triazol-5-one and Its Derivatives, *Bioinorg. Chemistry and Applications*. <https://doi.org/10.1155/2017/5237865> 15 pages.
  24. Reed, A. E., R. B. Weinstock, and F. Weinhold, 1985, Natural Population Analysis, *J. Chem. Phys.* **83**, 735-746.
  25. Singh, U. C., and P. A. Kollman, 1984. An Approach to Computing Electrostatic Charges for Molecules, *J. Comput. Chem.* **5**, 129-145.
  26. Breneman, C. M., and K. B. Wiberg, 1990. Determining Atom-Centered Monopoles from Molecular Electrostatic Potentials. The Need for High Sampling Density in Formamide Conformational Analysis, *J. Comput. Chem.* **11**, 361-373.
  27. Chirlian, L. E., and M. M. Francl, 1987. Atomic Charges Derived from Electrostatic Potentials: A Detailed Study, *J. Comput. Chem.* **8**, 894-905.
  28. Aakesson, R., L. G. M. Pettersson, M. Sandstroem, and U. Wahlgren, 1994, Ligand Field Effects in the Hydrated Divalent and Trivalent Metal Ions of the First and Second Transition Periods, *J. Am. Chem. Soc.* **116**, 8691-8704.
  29. Barone, V., and M. Cossi, 1998. Quantum Calculation of Molecular Energies and Energy Gradients in Solution by a Conductor Solvent Model, *J. Phys. Chem. A* **102**, 1995-2001.
  30. Tomasi, J., B. Mennucci, and R. Cammi, 2005. Quantum Mechanical Continuum Solvation Models, *Chem. Rev.* **105**, 2999-3094.
  31. Kasaei, G. A., D. Nori-Shargh, H. Yahyaei, S.N. Mousavi, E. Pourdavoodi, 2012. Complete basis set, hybrid-DFT study and NBO interpretation of conformational analysis of 2-methoxy tetrahydropyran and its thiopyran and selenopyran analogues in relation to the anomeric effect, *Molecular Simulation* **38 (12)**, 1022-1031.
  32. Thomson, H. W., P. Torkington, 1945. The vibrational spectra of esters and ketones, *J. Chem. Soc.* **171**, 640-645.

